Miniproteins

DOI: 10.1002/ange.201304603

A Disulfide-Constrained Miniprotein with Striking Tumor-Binding Specificity Developed by Ribosome Display**

*Frederic Zoller, Annette Markert, Philippe Barthe, Ulrike Hebling, Annette Altmann, Thomas Lindner, Walter Mier, and Uwe Haberkorn**

The lack of specificity of traditional cytotoxic drugs used in tumor therapies has triggered the astonishing advent of antibody therapeutics. However, these proteinaceous drugs suffer from poor pharmacokinetics.[1,2] Small molecules that are accessible by chemical synthesis and provide the same degree of specificity as those drugs are highly desired. Owing to their rigid framework, disulfide-constrained peptides offer the potential to achieve this binding capability.[3–5] To equip these miniproteins with a targeting specificity, libraries that present huge repertoires of random sequences have to be designed to evolve new molecular entities. This process is similar to the formation of highly specific antibodies by the immune system.

Several molecular screening techniques,[6] such as phage display,[7] yeast two-hybrid display,[8] and ribosome display,[8] have been developed. In ribosome display, the peptides presented for screening are linked to the corresponding random RNA through a ribosome, which provides high library diversity.[8,9] The binding peptides are identified by sequencing of the RNA. Figure 1 illustrates the screening cycle used in ribosome display.

Herein, ribosome display was used to identify miniproteins that bind to the delta-like ligand 4 (DLL4), a protein expressed in angiogenesis. As the growth of new capillary blood vessels is a prerequisite for tumor development,[10] antibodies that bind the vascular endothelial growth factor (VEGF), such as bevacizumab (Avastin, Genentech), have become established agents for angiogenic treatment.[11–13]

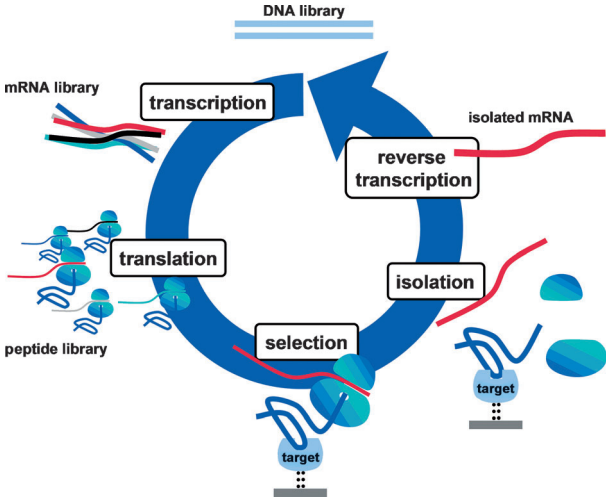

Figure 1. Ribosome-display selection cycle. A DNA library encoding different peptide motifs is transcribed. The resulting RNA sequences are translated and form the peptide–ribosome–mRNA complexes. In the selection step, the non-binding motifs are eliminated. The RNA sequences that are linked to peptide motifs with an affinity to the target are amplified and screened in the following repetitions of this selection process.

Its unique expression on the arterial endothelium makes DLL4 an alternative target for an anti-angiogenic approach,[14] both for the diagnosis and therapy of tumor angiogenesis.[15,16]

Recently, naturally occurring cystine-knotted peptides were exploited for the engineering of novel targeting agents for drug design[17] and molecular imaging.[18,19] The plant-derived cyclotide *Ecballium elaterium* trypsin inhibitor II (EETI-II) was applied in display libraries to identify specific integrin binders, and was used as an angiogenesis imaging tracer.[20,21]

Initially, a combinatorial scaffold library (Min-23R10) was designed for ribosome display where 10 amino acids were randomly inserted in the surface-exposed loop, between Cys^{16} and Cys^{28} of the Min-23 scaffold structure (Figure 2). This repertoire, with a theoretical diversity of 6×10^{13} peptides, was screened against the extracellular domain of recombinant DLL4. Min-23 is a rationally designed scaffold that was obtained by downsizing its parent knottin EETI-II,[22] and used as a scaffold to generate new recognition molecules by phage display[23] and artificial molecular evolution.[24] Recently, we reported a reliable chemical reaction pathway to Min-23;[25] its characteristics encouraged its use to generate

[*] Dr. F. Zoller,[+] Dr. A. Markert,[+] U. Hebling, Dr. A. Altmann
DKFZ, Klinische Kooperationseinheit Nuklearmedizin
Im Neuenheimer Feld 280, 69120 Heidelberg (Germany)
P. Barthe
Centre de Biochimie Structurale, Institut National pour la Santé et la Recherche Médicale U1054, Centre National pour la Recherche Scientifique Unité Mixte de Recherche 5048, Université Montpellier 1 and 2, 434090 Montpellier (France)
T. Lindner, Dr. W. Mier, Prof. U. Haberkorn
Universitätsklinikum Heidelberg, Radiologische Klinik, Abteilung Nuklearmedizin
Im Neuenheimer Feld 400, 69120 Heidelberg (Germany)
E-mail: uwe.haberkorn@med.uni-heidelberg.de
[+] These authors contributed equally to this work.

[**] The authors are grateful to the Bundesministerium für Bildung und Forschung (13N10269, 01EZ0807) and the Deutsche Forschungsgemeinschaft (HA 2901/6-1) for financial support. Support by Karin Leotta, Vasileios Askoxylakis, Ursula Schierbaum, Jennifer Melzer, Jessica Angel, Gabriela Glensch, Iris Wolf, and Eileen Gärtner is gratefully acknowledged. All animal experiments were carried out in accordance with the national animal guidelines.

Supporting information for this article, including detailed experimental methods, is available on the WWW under http://dx.doi.org/10.1002/anie.201304603.

a) H_2N-LMRCKQDSDCLAGSVCGPNGFCG-$CONH_2$

b) H_2N-LMRCKQDSDCLAGSVCXXXXXXXXXXFCG-COOH

c) H_2N-LXRCKQDSDCLAGSVC**GWYISNWAIH**FCG-COOH

Figure 2. a) Primary structure and disulfide connectivity of Min-23, b) the Min-23R10 display library containing ten random amino acids marked by X, c) the screening hit DLL-Rib identified by ribosome display. The binding domain (Gly-Trp-Tyr-Ile-Ser-Asn-Trp-Ala-Ile-His) is highlighted in bold; at position 2 norleucine substitutes methionine.

specific binders against DLL4. The compound identified was evaluated for diagnostic imaging using positron emission tomography (PET).

GWYISNAIWH, an anti-DLL4 binding domain (R10-Rib) that is displayed on the Min-23 scaffold, was identified after four biopanning cycles. The homology of this domain is shown in the Supporting Information, Figure S1. The entire construct, which presents the binding domain at the surface-exposed loop of the Min-23 scaffold, was named DLL-Rib.

The chain assembly of DLL-Rib was conducted by solid-phase peptide synthesis (Figure 3). The subsequent formation of the two disulfide bridges was performed by DMSO-mediated oxidative peptide folding in an ammonium acetate buffer that contained isopropanol and guanidinium hydrochloride to increase peptide solubility.[26] As already reported, the autonomous folding capability of Min-23 to form the native-like disulfide connectivity is highly affected by the integration of lipophilic amino acid residues into the random loop, which results in a mixture of different regioisomers.[23] Only 39% of the native-like (Cys^4-Cys^{16}/Cys^{10}-Cys^{28}) regioisomer was formed within 4 days of autonomous oxidative folding, as seen from the monitoring of the folding process, (Figure S2 and S3); precipitation of the reaction mixture reduced the yields. In contrast, the consecutive peptide folding that uses the orthogonal Cys(Acm)/Cys(Trt) protecting-group strategy,[25] yielded nearly exclusively the native-like configured regioisomer (Figure S5). HPLC-MS analysis confirmed the identical mass of the two peptides that were folded individually (Figure 4; Supporting Information, Table S1).

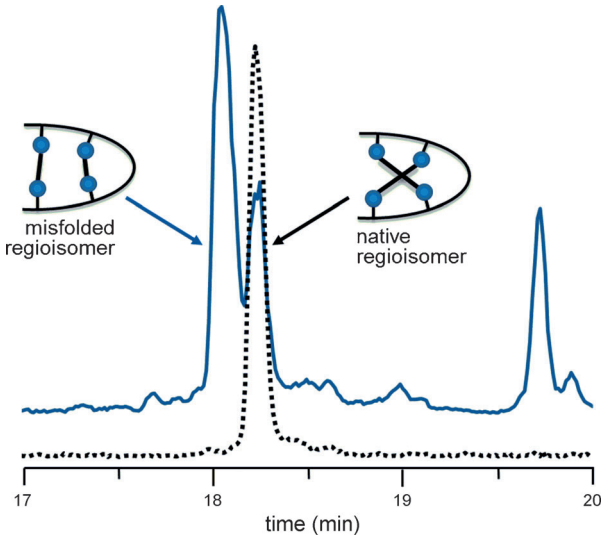

Figure 4. HPLC-MS analysis (crude reaction mixtures) of DLL-Rib. Autonomous oxidative folding results in the formation of two different regioisomers (upper trace), the consecutive folding exclusively yields the native regioisomer (lower trace).

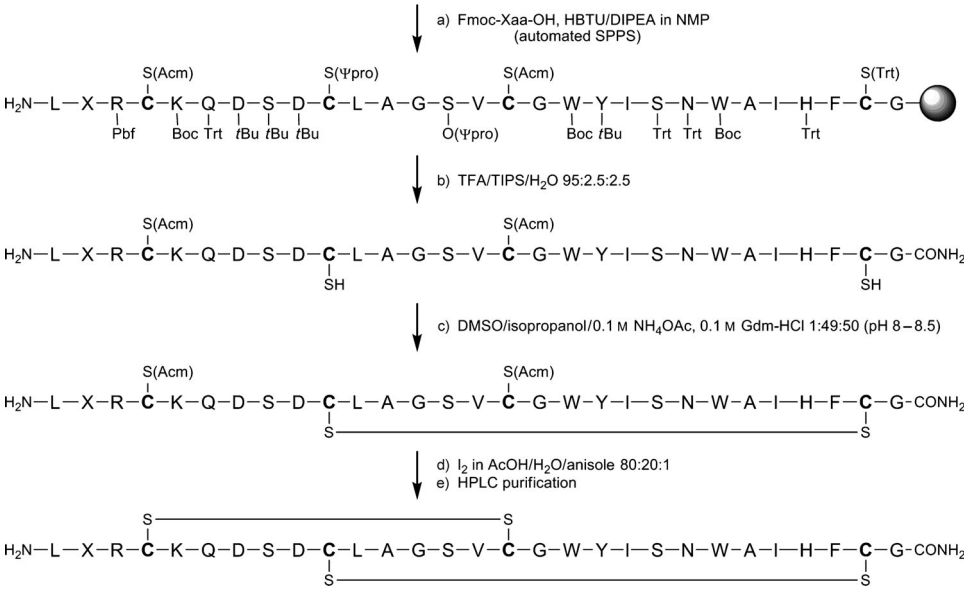

Figure 3. Synthesis of DLL-Rib. Oxidative folding of the miniprotein was performed using an orthogonal protecting-group strategy. The building block at position X^2 represents norleucine, used as a methionine substitute. Acm = acetamidomethyl, Boc = *tert*-butoxycarbonyl, DIPEA = diisopropylethylamine, Fmoc = 9-fluorenylmethyloxycarbonyl, Gdm = guanidinium, HBTU = *O*-(benzotriazol-l-yl)-*N*,*N*,*N*′,*N*′-tetramethyluronium hexafluorophosphate, NMP = *N*-methyl-2-pyrrolidinone, Pbf = 2,2,4,6,7-pentamethyldihydrobenzofuran-5-sulfonyl, SPPS = solid-phase peptide synthesis, Trt = triphenylmethyl, Ψpro = $\Psi^{H,DMP}$ pseudoproline (DMP = 2,4-dimethoxyphenyl).

The binding specificity of DLL-Rib was verified by surface plasmon resonance spectroscopy (SPR) using immobilized DLL4. The miniprotein that was generated by ribosome display demonstrated specific binding to DLL4 with nanomolar affinity (K_D = 44 nM). In comparison, the interaction of the misfolded regioisomer of DLL-Rib with

Structural assessment by NMR analysis unambiguously confirmed the cystine topology with a (Cys^4-Cys^{16}/Cys^{10}-Cys^{28}) connectivity (Figure 5). Detailed results for the miniprotein engineering, and the characterization are given in the Supporting Information.

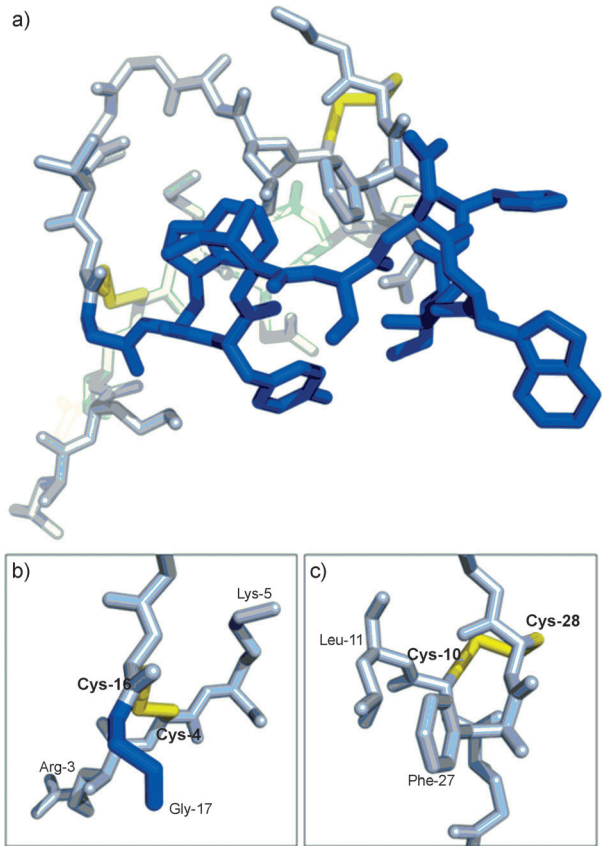

Figure 5. The solution structure, which was obtained by NMR analysis, of the engineered miniprotein DLL-Rib (a) shows the native-like disulfide connectivity between Cys^{4}-Cys^{16} (b) and between Cys^{10}-Cys^{28} (c). The variable surface-exposed loop is colored in blue, disulfide bridges are colored in yellow. Structural data were illustrated with the PyMol molecular visualization software. NMR spectroscopic data are given in the Supporting Information.

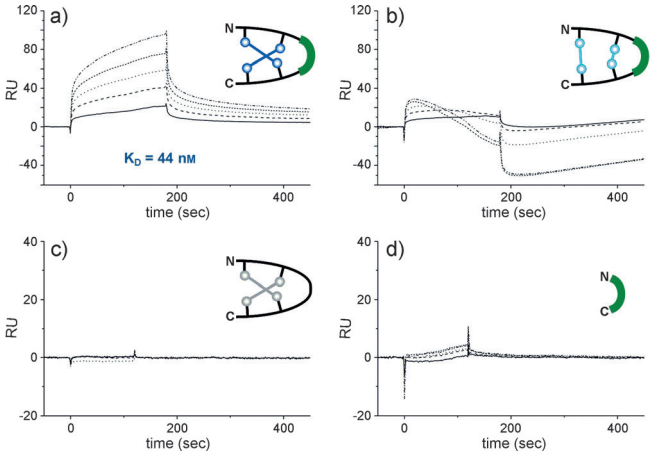

Figure 6. Binding specificity of engineered miniproteins. SPR senorgrams show the binding interaction of the identified miniprotein to immobilized DLL4 and to the reference compounds. The miniprotein DLL-Rib with native-like disulfide configuration (a) and with misfolded disulfide configuration (b), the unmodified scaffold Min-23 (c), and the isolated binding domain R10-Rib (d) are shown. RU = relative units.

the immobilized target was not recognized as specific binding. Moreover, the isolated binding domain R10-Rib and the unmodified Min-23 scaffold by itself did not interact specifically with the ligand (Figure 6). In a control experiment, the interaction of both DLL-Rib isomers with the immobilized Notch-1 receptor did not show specific binding (Figure S12).

The peptides were radiolabeled with different iodine isotopes to obtain the peptide tracers at radiochemical purities of $>95\,\%$, at specific activities of up to $26\,MBq\,nmol^{-1}$ (for iodine-124). Detailed radiochemical results are given in the Supporting Information.

The cell-binding capability of the radiolabeled DLL-Rib peptide was studied using human-umbilical-vein endothelial cells (HUVECs) and neuroendocrine pancreatic tumor cells (AR42J). The DLL4-expression of the selected cell lines was shown by western blot (Figure S13) and RT-PCR analysis. Natively folded DLL-Rib demonstrated the highest binding potential to both cell lines, with a maximum cell binding of $16.5\pm2.0\,\%$ on HUVECs and $5.1\pm0.7\,\%$ on AR42J. The misfolded miniprotein bound only with $9.8\pm0.5\,\%$ on HUVECs and with $3.3\pm0.5\,\%$ on AR42J; the isolated binding domain R10-Rib displayed a maximum binding of 7.3 ± 0.2 on HUVECs and $1.1\pm0.1\,\%$ on AR42J. The unmodified Min-23 scaffold did not show any relevant cellular binding capability. Only a minor fraction of the radiolabeled peptides was observed to be internalized (Figure S14).

The radiolabeled miniprotein ^{125}I-(Tyr^{19})DLL-Rib demonstrated a high stability in human serum with an estimated half-life of 20 h (Figure S15).

The iodine-131 labeled peptides were intravenously injected into AR42J tumor-bearing mice (the presence of endothelial cells in AR42J tumor tissue, which indicates neovascularization, was confirmed by anti-CD31 staining of AR42 J tumor cryosections (Figure S16)). The tracer showed a rapid accumulation of $3.31\pm0.86\,\%$ ID/g (percent injected dose per gram) in the tumor 10 min post-injection (p.i.). This value increased to a maximum of $3.93\pm0.93\,\%$ ID/g after 60 min. Although the accumulation in the tumor was of high retention, no persistent accumulation in the non-specific compartments, such as the heart, lung, or the muscles was observed (Figure 7a; see also the Supporting Information, Figure S18). The tumor was the only tissue of interest that showed a continuous uptake over a period of two hours after tracer administration. The clearance from the non-specific compartments resulted in a maximum tumor-to-muscle ratio of 9.74 ± 1.19 and a tumor-to-blood ratio of 2.18 ± 0.32 at 120 min p.i. (Table S5).

Co-administration of excess unlabeled DLL-Rib resulted in a reduced tumor uptake of $1.71\pm0.37\,\%$ ID/g 120 min p.i. (46% inhibition), which confirmed the in vivo binding specificity to DLL4 (Figure 7b). The control peptides, misfolded DLL-Rib and the native Min-23 scaffold, demonstrated a tumor uptake of $1.28\pm0.32\,\%$ ID/g and $0.85\pm0.27\,\%$ ID/g, respectively, at 120 min p.i. (Table S6). The specific tumor uptake of ^{124}I-(Tyr^{19})DLL-Rib was proven using small-animal PET. The tumor lesion was delineated instantly after tracer administration, and persisted over the course of the observation, while the initial accumulation in the liver decreased (Figure 8).

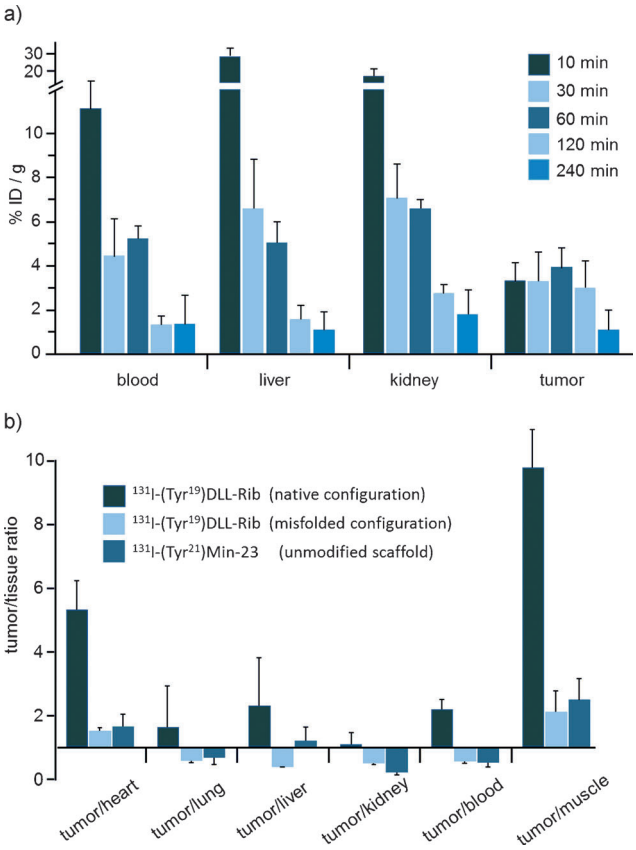

Figure 7. Biodistribution of ^{131}I-(Tyr^{19})DLL-Rib in AR42J tumor-bearing mice. a) Radioactivity concentrations in selected organs (%ID/g) measured after 10, 30, 60, 120 and 240 min p.i. in mice ($n=3$ per group; mean ± SD). b) Tumor-to-organ ratios in AR42J tumor-bearing mice ($n=3$ per group) of ^{131}I-(Tyr^{19})DLL-Rib, and administration of the iodine-131 labeled misfolded regioisomer and ^{131}I-(Tyr^{21})Min-23 as controls at 120 min. p.i. ($n=3$ per group; mean ± SD).

As a consequence of the successes achieved with tumor targeting peptides,[27,28] small constrained peptides have been studied to gain access to peptides with favorable in vivo properties. Pioneering work has been done by Kimura et al.,[21] who studied RGD-motifs.

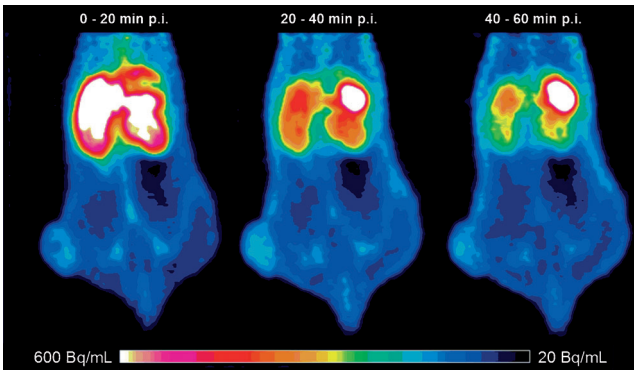

Figure 8. Coronal PET images of dynamic PET-images in an AR42J tumor-bearing rat after injection of 25 MBq of ^{124}I-(Tyr^{19})DLL-Rib. The tumor lesion is marked. Summation images over 20 min frames.

The peptide described herein displayed an impressive specificity, but only at double-digit nanomolar affinity, and thus the peptide does not yet attain the remarkable binding characteristics of the RGD based peptides that could be even further improved.[29] Despite these favorable binding characteristics, the potential of the limited group of known peptides is restricted, and significant innovations could be achieved by the de novo discovery of peptide sequences.

In conclusion, by conducting ribosome display with a custom-made Min-23 scaffold library, we were able to identify a novel miniprotein that binds DLL4 with nanomolar affinity. Solid phase peptide synthesis and regioselective cysteine formation were applied to synthesize this novel Min-23 derivative. As demonstrated in different assay systems, a specific DLL4-targeting was only shown for the native-like folded miniprotein with a (Cys^4-Cys^{16}/Cys^{10}-Cys^{28}) linkage. Consistently, the distinct bioactivity of the two different regioisomers of DLL-Rib revealed a mutual behavior in independent assay systems, conducted both in vitro and in vivo. These results accentuate the potential of DLL-Rib generated by ribosome display as a molecular diagnostic agent in cancer research.

Received: May 28, 2013
Revised: July 17, 2013
Published online: September 20, 2013

Keywords: molecular imaging · peptide folding · protein design · ribosome display · solid-phase synthesis

[1] M. M. Schmidt, K. D. Wittrup, *Mol. Cancer Ther.* **2009**, *8*, 2861.
[2] S. K. Batra, M. Jain, U. A. Wittel, S. C. Chauhan, D. Colcher, *Curr. Opin. Biotechnol.* **2002**, *13*, 603.
[3] A. Skerra, *Curr. Opin. Biotechnol.* **2007**, *18*, 295.
[4] H. K. Binz, P. Amstutz, A. Pluckthun, *Nat. Biotechnol.* **2005**, *23*, 1257.
[5] F. Zoller, U. Haberkorn, W. Mier, *Molecules* **2011**, *16*, 2467.
[6] A. Marr, A. Markert, A. Altmann, V. Askoxylakis, U. Haberkorn, *Methods* **2011**, *55*, 215.
[7] G. P. Smith, V. A. Petrenko, *Chem. Rev.* **1997**, *97*, 391.
[8] B. Dreier, A. Plückthun, *Methods Mol. Biol.* **2011**, *687*, 283.
[9] J. Hanes, A. Plückthun, *Proc. Natl. Acad. Sci. USA* **1997**, *94*, 4937.
[10] D. Hanahan, R. A. Weinberg, *Cell* **2011**, *144*, 646.
[11] L. M. Ellis, D. G. Haller, *J. Clin. Oncol.* **2008**, *26*, 5313.
[12] A. Grothey, L. M. Ellis, *Cancer J.* **2008**, *14*, 170.
[13] A. Grothey, E. Galanis, *Nat. Rev. Clin. Oncol.* **2009**, *6*, 507.
[14] D. J. Hicklin, *Nat. Biotechnol.* **2007**, *25*, 300.
[15] I. Noguera-Troise, C. Daly, N. J. Papadopoulos, S. Coetzee, P. Boland, N. W. Gale, H. Chieh Lin, G. D. Yancopoulos, G. Thurston, *Nature* **2006**, *444*, 1032.
[16] T. Hoey, W. C. Yen, F. Axelrod, J. Basi, L. Donigian, S. Dylla, M. Fitch-Bruhns, S. Lazetic, I. K. Park, A. Sato, S. Satyal, X. Wang, M. F. Clarke, J. Lewicki, A. Gurney, *Cell Stem Cell* **2009**, *5*, 168.
[17] N. L. Daly, D. J. Craik, *Curr. Opin. Chem. Biol.* **2011**, *15*, 362.
[18] H. Kolmar, *Expert Rev. Mol. Diagn.* **2010**, *10*, 361.
[19] F. Zoller, A. Markert, P. Barthe, W. Zhao, W. Weichert, V. Askoxylakis, A. Altmann, W. Mier, U. Haberkorn, *Angew. Chem.* **2012**, *124*, 13313; *Angew. Chem. Int. Ed.* **2012**, *51*, 13136.
[20] H. Kolmar, *FEBS J.* **2008**, *275*, 2684.
[21] R. H. Kimura, Z. Cheng, S. S. Gambhir, J. R. Cochran, *Cancer Res.* **2009**, *69*, 2435.

[22] A. Heitz, D. Le-Nguyen, L. Chiche, *Biochemistry* **1999**, *38*, 10615.
[23] C. Souriau, L. Chiche, R. Irving, P. Hudson, *Biochemistry* **2005**, *44*, 7143.
[24] H. J. Chang, H. J. Hsu, C. F. Chang, H. P. Peng, Y. K. Sun, H. M. Yu, H. C. Shih, C. Y. Song, Y. T. Lin, C. C. Chen, C. H. Wang, A. S. Yang, *Structure* **2009**, *17*, 620.
[25] F. Zoller, T. Schwaebel, A. Markert, U. Haberkorn, W. Mier, *ChemMedChem* **2012**, *7*, 237.
[26] B. Kamber, A. Hartmann, K. Eisler, B. Riniker, H. Rink, P. Sieber, W. Rittel, *Helv. Chim. Acta* **1980**, *63*, 899.
[27] H. R. Maecke, M. Hofmann, U. Haberkorn, *J. Nucl. Med.* **2005**, *46 Suppl 1*, 172S.
[28] J. C. Reubi, *Endocr. Rev.* **2003**, *24*, 389.
[29] R. H. Kimura, R. Teed, B. J. Hackel, M. A. Pysz, C. Z. Chuang, A. Sathirachinda, J. K. Willmann, S. S. Gambhir, *Clin. Cancer Res.* **2012**, *18*, 839.